

Attacking Point Cloud Segmentation with Color-only Perturbation

Jiacen Xu¹, Zhe Zhou², Boyuan Feng³, Yufeng Ding³, Zhou Li¹,

¹University of California, Irvine

²Fudan University

³University of California, Santa Barbara

jiacenx@uci.edu, zhouzhe@fudan.edu.cn, {boyuan, yufeiding}@ucsb.edu, zhou.li@uci.edu

Abstract

Recent research efforts on 3D point-cloud semantic segmentation have achieved outstanding performance by adopting deep CNN (convolutional neural networks) and GCN (graph convolutional networks). However, the robustness of these complex models has not been systematically analyzed. Given that semantic segmentation has been applied in many safety-critical applications (e.g., autonomous driving, geological sensing), it is important to fill this knowledge gap, in particular, how these models are affected under adversarial samples. While adversarial attacks against point cloud have been studied, we found all of them were targeting single-object recognition, and the perturbation is done on the point coordinates. We argue that the coordinate-based perturbation is unlikely to realize under the physical-world constraints. Hence, we propose a new color-only perturbation method named COLPER, and tailor it to semantic segmentation. By evaluating COLPER on an indoor dataset (S3DIS) and an outdoor dataset (Semantic3D) against three point cloud segmentation models (PointNet++, DeepGCNs, and RandLA-Net), we found color-only perturbation is sufficient to significantly drop the segmentation accuracy and aIoU, under both targeted and non-targeted attack settings.

Introduction

3D point cloud segmentation aims to assign a class label to each embedded 3D point in a scene. It has been playing an increasingly important role in many real-world applications, like autonomous driving and geological sensing. Due to the data complexity, deep-learning models based on CNN and GCN have been extensively leveraged for this task (Li et al. 2019a; Landrieu and Martin 2018; Wei et al. 2020). However, the robustness of these models under the adversarial samples have not been systematically explored, leaving doubts on its deployment for safety-critical applications.

Prior Attacks on Point Cloud. Existing works on generating adversarial examples for point cloud focus on the task of *single-object recognition*, in which a class label is assigned to the whole point cloud. The methods based on adversarial perturbation for 2D images, like FGSM, iFGSM, PGD and C&W, were applied by the prior works (Yang et al. 2019; Xiang, Qi, and Li 2019; Zhou et al. 2020a; Liu,

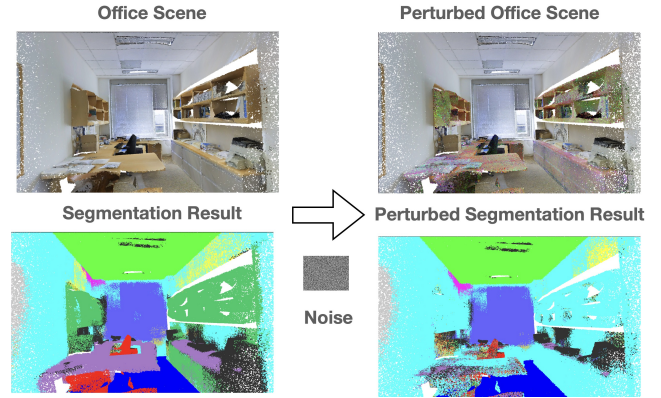


Figure 1: One example of S3DIS dataset after color-only perturbation under the targeted attack setting. Different objects are colored differently. Multiple objects (desk, chair, and bookcase) are misclassified after the attack.

Yu, and Su 2019; Wicker and Kwiatkowska 2019; Cai et al. 2020; Kim et al. 2020).

However, the task of *semantic segmentation* has not been examined under the adversarial settings. In fact, a few challenges prohibit the direct usage of the existing attack methods. First, in the segmentation task, the class label is assigned to *every* point, and the segmentation result of a point is also determined by its surrounding points, which increases the uncertainty of the attack outcome. Second, the existing attacks assume the point coordinates can be changed or new points can be added. When converting the adversarial sample to a physical instance, such assumption is acceptable under object recognition, as only one object needs to be considered, e.g., being created against LiDAR (Tu et al. 2020; Cao et al. 2019; Li et al. 2019b). Doing so against semantic segmentation is unclear, given the complex interplay between objects in the same scene, and various data preprocessing procedures such as random filtering, nodes copying, and point clouds separation. Finally, perturbation is only performed on the point coordinates by prior works, but there are other point features are used for semantic segmentation. For instance, 9 features are included in a point cloud of the S3DIS dataset (Xu et al. 2020) and 6 features are included in Semantic3D dataset (Hackel et al. 2017). Whether and how

the features undermine the robustness of the segmentation models have not been studied.

Our Method. We perform the first systematic analysis on the robustness of point cloud segmentation, by addressing the aforementioned challenges. Our key observation is that color is usually contained in the feature set of a point cloud and used by segmentation model, and it is much easier to manipulate (only three channels and each channel is ranged in $[0, 255]$) and realize physically (*e.g.*, by attached a printed sticker to the targeted object). Hence, we propose a color-only perturbation method, termed COLPER, for this work. In particular, we first formally define the goals of the targeted and non-targeted attacks in point cloud segmentation and convert them to the form that can be solved through optimization. Then, we tailor the existing loss and distance functions to our optimization problem, and design an algorithm for the gradient-based test-time white-box attack.

Evaluation Results. We evaluate COLPER on three point cloud models, PointNet++ (Qi et al. 2017b), ResGCN-28 (Li et al. 2019a), and RandLA-Net (Hu et al. 2020) on point clouds from S3IDS and Semantic3D, for both targeted and non-targeted attack. Here we highlight the key results. **(1)** By only perturbing the color, the accuracy and average IoU of semantic segmentation drop significantly for the non-targeted attack, *e.g.*, from 85.90% to 6.75% for the accuracy of ResGCN-28. In the meantime, the noise added to the original point cloud is insignificant. Notably, PointNet++, ResGCN-28 and RandLA-Net belong to very different model families, and S3IDS and Semantic3D are about very different scenes (indoor vs outdoor) suggesting COLPER could be universally effective. **(2)** For non-targeted attack, we found some classes are easier to manipulate (*e.g.*, changing board to wall in S3IDS) while some are not. Figure 1 shows an example of the targeted attack. **(3)** We compare the perturbation on color against coordinates, and our result shows the color feature are more vulnerable under the attacks. **(4)** The adversarial examples generated against one model have good transferability against another model with different parameters or even from different families. Our study demonstrates that the robustness of the deep-learning models under point cloud segmentation is questionable, and we outline a few directions for improving their robustness.

Background and Related Works

Deep Learning on Point Cloud

To process a point cloud, early works transformed the data representation into regular 3D voxel grids or images for the conventional CNN, which makes the data unnecessarily voluminous. PointNet (Qi et al. 2017a) addressed this issue by using a shared MLP on every individual point, and a global max-pooling to convert the input into a fixed-length feature vector. Since then, variations like PointNet++ (Qi et al. 2017b), So-net (Li, Chen, and Hee Lee 2018), PointCNN (Li et al. 2018), KPConv (Thomas et al. 2019) have been proposed to use hierarchical architectures to aggregate local neighborhood information while COLPER will be firstly evaluated on PointNet++.

Besides CNN, DeepGCN (Li et al. 2019a) shows that GCN can be leveraged to handle point cloud, as the data is sparse in the geometry space but nodes in adjacency have strong relations. Hence, we also choose DeepGCN as an evaluation target. A major drawback of many point cloud models is that the pre-processing and voxelization steps are too computation-intensive for large point clouds. To address this issue, RandLA-Net (Hu et al. 2020) leveraged random point sampling and local feature aggregation, and showed 200× speedup. The large outdoor dataset like Semantic3D can be handled efficiently. Hence, we use RandLA-Net as an example on attacking outdoor datasets. Recently, other deep models like GAN (Shu, Park, and Kwon 2019) and transformer (Zhao et al. 2020; Mazur and Lempitsky 2020) have been leveraged for semantic segmentation. We leave the evaluation on them as a future work.

Adversarial Examples

The output of a point cloud model can be manipulated under adversarial examples. In the setting of 3D point cloud, existing works (Yang et al. 2019; Xiang, Qi, and Li 2019; Zhou et al. 2020a; Liu, Yu, and Su 2019; Wicker and Kwiatkowska 2019; Zheng et al. 2019; Xie et al. 2017) usually took a gradient-based approach to generate adversarial examples by perturbing the coordinates of a point or adding/removing a point. GAN has also been used to create adversarial examples (Zhou et al. 2020b). The popular methods in attacking CNN that handles 2D images, including FGSM (Goodfellow, Shlens, and Szegedy 2014), iFGSM (Kurakin, Goodfellow, and Bengio 2016), PGD (Madry et al. 2017), and C&W (Carlini and Wagner 2017), have been applied. However, these works aim to fool object recognition. For semantic segmentation, the existing works (Arnab, Miksik, and Torr 2018) generate adversarial examples on 2D images. Therefore, the robustness of deep-learning based semantic segmentation on 3D point cloud has not been systematically evaluated. In this paper, we make the *first* attempt to fill this knowledge gap.

Problem Formulation

A point cloud can be defined as a set of N points, *i.e.*, $\{p_i\}_{i=1}^N$ where each point $p_i = (pos_x, pos_y, pos_z)$ and $p_i \in R^3$, representing the 3D coordinates of a point. This basic form is usually sufficient for single-object recognition (Qi et al. 2017a,b). For semantic segmentation, auxiliary features of a point like color are also leveraged, which can be obtained from a multi-spectral LiDAR. In this work, we assume a point has three color channels in addition to coordinates, so a point cloud $X = \{x_i | i = 1 \dots N, x_i = \{p_i, c_i\}\}$ where $c_i = (color_r, color_g, color_b)_{i=1 \dots N}$. The three color channels represent red, green and blue strength respectively, and $color_*$ is the pixel value that ranges in $[0, 1]$ normalized from $[0, 255]$.

Perturbing the point coordinates at pixel granularity of an object in the physical world is very challenging (Cao et al. 2019; Tu et al. 2020). In contrast, changing the color of an object should be easier in the physical world, *e.g.*, through pasting carefully-printed stickers on the surface (Eykholt

et al. 2018). Even when factors like the surrounding illuminations, viewing angle and distance are considered, previous works show that pasting stickers can generate robust examples (Eykholt et al. 2018; Zhao et al. 2019).

We assume the adversary has white-box access to the model to be attacked. In other words, the adversary has full access to the model’s structure and parameters. The perturbation happens on the model input in the test time. We study two types of attack: *targeted* attack and *non-targeted* attack. Below we formalize their goals. Firstly, we assume $F_\theta : \mathcal{X} \leftrightarrow \mathcal{Y}$ is the segmentation model which maps an input point cloud $X = \{x_i | i = 1 \dots N, x_i \in \mathcal{X}\}$ to the labels of *all points* $Y = \{y_i | i = 1 \dots N, y_i \in \mathcal{Y}\}$. \mathcal{Y} is the set of object labels, e.g., desk, wall and chair. Table 5 from the supplementary material lists the symbols and their description.

Targeted Attack. In this setting, the adversary chooses a subset of points $X_t = \{x_i | i \in T, x_i \in X\}$, where T is the set of indices, and perturbs X_t to change their predicted labels to Y_t ($Y_t = \{y_i | i \in T, y_i \in \mathcal{Y}\}$). Since we limit the perturbation on the color channels, the adversarial changes can be represented as $r_{color} = \{\hat{c}_i | i \in T\}$. And the new point cloud will be $X' = \{x_i | i \notin T, x_i \in X\} + \{x'_i = x_i + \{0^3, \hat{c}_i\} | i \in T, x_i \in X\}$. The attacker’s goal can be formalized as:

$$\begin{aligned} & \arg \min_{r_{color}} \mathcal{D}(r_{color}) \\ & \text{subject to } \mathbf{F}_\theta(X') = Y_t \end{aligned} \quad (1)$$

Here, $\mathcal{D}(\cdot)$ is the distance function measuring the magnitude of the perturbation of r_{color} . Notably, the attacker’s goal is quite different from the attacks against single-object recognition (e.g., Equation 1 of (Xiang, Qi, and Li 2019)), where one label is assigned to the whole point cloud (i.e., the cardinality of Y_t is 1) and the number of points after perturbation can differ (i.e., X' and X have different cardinalities).

Directly solving Equation 1 is difficult as pointed out by (Carlini and Wagner 2017). As a result, we reformulate Equation 1 to enable gradient-based optimization by introducing a loss item encoding the constraint, as shown in Equation 2. Besides, we add a smoothness penalty $\mathcal{S}(X')$ to encourage the optimizer to keep X' smooth, i.e., that the differences between the neighboring points are not drastic.

$$\arg \min_{r_{color}} \mathcal{D}(r_{color}) + \lambda_1 \cdot \mathcal{L}_t(X', Y_t) + \lambda_2 \cdot \mathcal{S}(X') \quad (2)$$

Where $\mathcal{L}_t(\cdot)$ is the adversarial loss, and λ_1 and λ_2 are constant values.

Non-targeted Attack. In this setting, the adversary does not have a specific target Y_t , but just manipulates the prediction $\mathbf{F}_\theta(X')$ to be different from the ground-truth labels of all points in X_t (termed Y_{gt}). Then, the attacker’s goal becomes:

$$\arg \min_{r_{color}} \mathcal{D}(r_{color}) + \lambda_1 \cdot \mathcal{L}_{nt}(X', Y_{gt}) + \lambda_2 \cdot \mathcal{S}(X') \quad (3)$$

Where $\mathcal{L}_{nt}(\cdot)$ is the adversarial loss regarding Y_{gt} .

Our Attack COLPER

We designed a novel color-constrained perturbation method termed COLPER to attack 3D point cloud semantic segmentation. Following the Equation 1, we define our distance function $\mathcal{D}(\cdot)$, adversarial loss item \mathcal{L} and smoothness penalty below.

Distance Function. We use L_2 distance to measure the magnitude of the perturbation, as shown by Equation 4. Notably, (Xiang, Qi, and Li 2019) uses a more complex Chamfer distance to measure the point-wise distance. The Chamfer distance is not selected here because no point is removed or added and the computation on L_2 distance is fast.

$$\mathcal{D}(r_{color}) = \sum_{\hat{c}_i \in r_{color}} \|\hat{c}_i\|_2^2 \quad (4)$$

We design a new mapping function to replace the perturbed feature $c_i \in [a, b]$ to a new variable W_i which has the same number of dimensions as r_{color} and perform optimization over W_i , as shown in Equation 5. Here $\tanh(\cdot)$ makes the gradient smoother, so the optimizer may find the right perturbation sooner continuously. Besides, $\tanh(\cdot)$ guarantees that the generated color perturbation will not exceed the valid range in the iterative process. We set a and b to 0 and 1 for color, and they can be adjusted for other features.

$$\hat{c}_i = a + \frac{b-a}{2} (\tanh(W_i) + 1) \quad (5)$$

Smoothness Penalty. The penalty is designed to make X' smooth. In Equation 6, the distance between each point and its top α nearest neighbors is encouraged to be minimized.

$$\mathcal{S}(X', \alpha) = \sum_{x'_i \in X'} \sum_{x'_j \in NB(x'_i, \alpha)} (\|x'_i - x'_j\|_2) \quad (6)$$

Where $NB(x'_i, \alpha)$ returns the top α nearest neighbors.

Adversarial Loss. We use the logits (the output of the layer before the last softmax layer) of F_θ to represent the adversarial loss for the targeted attack. This loss encourages the optimizer to minimize the logits of the class rather than the target label.

$$\mathcal{L}_t(X', Y_t) = \sum_{\substack{x'_i \in X' \\ y_i \in Y_t}} \max(\max_{j \neq y_i} (Z(x'_i)_j) - Z(x'_i)_{y_i}, 0) \quad (7)$$

Where $Z(\cdot)_j$ represents the j^{th} element of the logits of the adversarial example, and $Z(x'_i)_t$ means the target label’s logits for x'_i .

For the non-targeted attacks, the adversarial loss is adapted to encourage the prediction of the points to be any class other than the ground-truth classes. The other items are the same as the targeted attacks.

$$\mathcal{L}_{nt}(X', Y_{gt}) = \sum_{\substack{x'_i \in X' \\ y_{gt} \in Y_{gt}}} \max(Z(x'_i)_{y_{gt}} - \max_{j \neq y_{gt}} (Z(x'_i)_j), 0) \quad (8)$$

Algorithm 1 summarizes the workflow of COLPER, which performs optimization iteratively under the goals defined in Equation 2 and 3, till one termination condition is

Algorithm 1: The pseudo-code of COLPER .

Input: the original point cloud X , the ground-truth labels Y_{gt} , the maximal number of iterations $Steps$, the target labels Y_t , the top α nearest neighbors, the learning rate lr , the constant λ_1, λ_2

Output: the adversarial perturbation r_{color}

$X_0 \leftarrow X, r \leftarrow X^{color}, i \leftarrow 1;$

$w = \tanh^{-1}(2r - 1);$

while $i \leq Steps$ **do**

$X_i^{color} = \frac{1}{2} \tanh(w) + 1;$

$r = X_i^{color} - X_{i-1}^{color};$

$X_i = X_{i-1} + r;$

$dist = \mathcal{D}(r);$

$smooth = \mathcal{S}(X_i);$

if *targeted attack* **then**

$loss = \mathcal{L}_t(X_i, Y_t);$

else if *non-targeted attack* **then**

$loss = \mathcal{L}_{nt}(X_i, Y_{gt});$

$gain_i = dist + \lambda_1 \cdot loss + \lambda_2 \cdot smooth;$

$r_{color} = Update(gain_i, lr);$

if *Converge*($gain_i$) **then**

return $r_{color};$

else if $(i \% (int(Steps * 0.01))) == 0$ &

$(gain_i \geq gain_{i-1})$ **then**

$r_{color} = r_{color} + \text{uniform noise};$

$i \leftarrow i + 1;$

end

return $r_{color};$

met. We set an upper-bound of iterations as $Steps$. In each step, the gain over the targeted attack or the non-targeted attack is examined by *Converge* to determine if the adversarial example is satisfactory, based on attacker’s evaluation metrics, *e.g.*, the dropped accuracy. If the gain does not increase in 10 steps, the perturbation will add random noise following the uniform distribution in $(0, 1)$. When the adversarial example is invalid, *e.g.*, $X_i^{color} \notin [0, 1]^3$, a new noise will replace the previous one. In Section , the hyper-parameter values used for evaluation are described.

Attack Evaluation

Experiment Settings

Target Models. We use the pre-trained PointNet++ (Qi et al. 2017b), ResGCN-28 under the DeepGCN family (Li et al. 2019a), and RandLA-Net (Hu et al. 2020) as the target models to evaluate COLPER , mainly because their codes and pre-trained models are publicly available. The links of the source code are in the supplementary materials.

PointNet++ consists of 4 abstraction layers and 4 feature propagation layers with 1 voter number. The overall point accuracy and average IoU (aIoU) of the pre-trained PointNet++ on the indoor dataset S3DIS are 82.65% and 70.71% respectively, as reported in the GitHub repo. ResGCN-28 uses dynamically dilated k -NN and residual graph connec-

tions, and the pre-trained model configures k to 16. It has 64 filters and 28 blocks with 0.3 drop-out rate and 0.2 stochastic epsilon for GCN. The accuracy and aIoU of the pre-trained ResGCN-28 model on S3DIS are 85.9% and 79.72%, as reported in the GitHub repo. The pre-trained RandLA-Net downsamples large point clouds. Its accuracy and mIoU are 88.0% and 82.0% on S3DIS, and 94.8% and 77.4% on the outdoor dataset Semantic3D .

Dataset. We evaluate COLPER on two large-scale 3D datasets: an indoor dataset S3DIS and an outdoor dataset Semantic3D. They have been extensively used as the benchmark for point cloud semantic segmentation.

The S3DIS dataset is composed of 3D point clouds with color channels, which were collected at 6 areas in 3 different buildings with 13 class labels. Each point cloud contains 4,096 points, and each point has 9 features. The point cloud data could be pre-processed differently by their segmentation models. As for PointNet++, each point cloud is segmented into several parts, and the coordinate and color are normalized to $[0, 3]$ and $[0, 1]$. As for ResGCN-28, the coordinate is normalized to $[-1, 1]$ while the color feature is normalized to $[0, 1]$. RandLA-Net regenerates the point clouds with 40,960 points by randomly duplicating and selecting the points. The color feature is also normalized to $[0, 1]$. For the non-targeted attack on S3DIS, we evaluate against the three models with the point clouds of Area 5. For the targeted attack, we selected the 100 point clouds in Office 33 of Area 5 when evaluating against PointNet++ and ResGCN-28. As RandLA-Net has different requirement of point number, for each class (*e.g.*, table), we randomly selected 100 point clouds in Area 5 which at least contains 500 points in the class.

The Semantic3D dataset contains 30 point clouds including coordinates, color channels, and intensity in 8 classes. Each point cloud has over 10^8 points to compose a $160 \times 240 \times 30 m^3$ area. PointNet++ and ResGCN-28 are not designed to handle such big point clouds, so we evaluate against RandLA-Net for both non-target and target attack.

Evaluation Metrics. We use the drop of accuracy and aIoU as the indicators of the attack effectiveness. On a point cloud sample, accuracy and aIoU are defined as follows. Assuming the number of all points and correctly classified points are N and TP , accuracy equals to $\frac{TP}{N}$. For a class i , IoU is defined as $\frac{TP_i}{FN_i + FP_i + TP_i}$, where FN_i, FP_i, TP_i are the number of false negatives, false positives and true positives for the class-related points. Below, we will primarily show the accuracy and aIoU averaged over point clouds.

For the targeted attack, the drop of accuracy and aIoU only measure whether the classification results are changed, but they neglect whether the predictions are misled toward the target classes. Therefore, we define another metric, *success rate (SR)*, as the ratio of the points that are correctly fooled over all the attacked points in X_t . We are also interested in whether the segmentation results of points outside of X_t are changed, so we compute the accuracy and aIoU on the subset of these points separately, and call the metrics “*out-of-band*” (*OOB*) accuracy and aIoU.

Hyper-parameters of COLPER . We set $Steps$ to 1,000.

Case		Baseline			COLPER		
		L_2	Accuracy	aIoU	L_2	Accuracy	aIoU
PointNet++	Best	2.68	14.51%	14.26%	2.68	4.91%	2.31%
	Average	18.19	77.26%(5.39%↓)	70.02%(0.69%↓)	18.27	7.86% (74.79%↓)	8.85% (61.86%↓)
	Worst	30.02	100%	100%	30.03	20.33%	59.27%
ResGCN-28	Best	1.29	7.79%	4.11%	1.29	0.31%	0.16%
	Average	4.30	82.36%(3.54%↓)	73.17%(6.55%↓)	4.30	6.75% (79.15%↓)	3.49% (76.23%↓)
	Worst	9.81	100%	100%	9.81	18.34%	10.10%
RandLA-Net	Best	6.65	34.07%	12.56%	6.65	6.13%	0.92%
	Average	17.06	78.01%(6.24%↓)	44.82%(6.6%↓)	17.06	7.45% (76.75%↓)	2.96% (48.45%↓)
	Worst	54.62	97.18%	70.08%	54.62	7.69%	8.33%

Table 1: The results of the non-targeted attack from PointNet++, ResGCN-28, and RandLA-Net on S3DIS.



Figure 2: The upper figures show the perturbed scene of Office 33 of Area 5 in S3DIS. The lower figures display the segmentation result of the perturbed point clouds.

Both λ_1 and λ_2 are set to 1 based on empirical analysis. The Adam optimizer with 0.01 learning rate is used. α is set to 10. The batch sizes of COLPER are set to 8 when attacking PointNet++ while to 1 when attacking ResGCN-28 and RandLA-Net. For the targeted attack, the adversarial example is considered satisfactory when SR is above 95%. For the non-targeted attack, we examine whether the accuracy is dropped below 7.6% (i.e., 1/13) for S3IDS and 12.5% (i.e., 1/8) for Semantic3D, which means the model’s prediction is the same as random guessing.

Experiment Platform. We run the experiments on a workstation with an Intel i9-9900K CPU and two Nvidia RTX 2080ti GPUs (10GB GPU memory). COLPER runs on PyTorch 1.7.1 for the pre-trained PointNet++ and ResGCN-28, and Tensorflow 1.15 for the pre-trained RandLA-Net.

Evaluation Results on S3IDS

Non-targeted Attack. As described in Section , the attacker’s goal is to change the prediction results of points in X_t . Here we visualize the attack outcome with one example, and we assume PointNet++ is the target model. From Figure 2, The original scene of Office 33 of Area 5 is shown in the upper left and the lower left one is its corresponding segmentation result. We consider X_t as all the points in the point cloud, and apply COLPER . The segmentation result

is changed to the lower right figure. For instance, the points related to the desk at the bottom left are mis-classified as a bookcase. As the two upper figures from Figure 2 shows, their difference is insignificant.

In Table 1, we show the comparison of the accuracy and aIoU across the tested point clouds (“best” and “worst” show the examples most vulnerable and robust against the attack). We also show the L_2 distance between the original point cloud and the perturbed version. It turns out COLPER can *drastically* reduce both accuracy and aIoU, e.g., **dropping the accuracy of PointNet++, ResGCN-28, and RandLA-Net from 82.65% to 7.86%, 85.90% to 6.75%, and 87.2% to 7.45% separately**, suggesting color-only perturbation is sufficient. As a baseline to compare against, we implemented another perturbation approach that adds random noises to the color channels under the similar L_2 distance of COLPER . It turns out all three models are robust against the baseline attack, with the drop of the average accuracy being around 6%. The result suggests successful attack is non-trivial.

In Figure 3 and Figure 4, we show the L_2 distance, accuracy and aIoU of each point cloud and draw their distributions after the attack on PointNet++ and ResGCN-28. We do not consider RandLA-Net in the analysis due to the differences in data pre-processing. The y-axis of each figure is the number of point clouds. “clean” and “adv” mean the results before and after our attack. We found that the accuracy and aIoU after the attack are *consistently below 20%*, showing COLPER is effective across samples. In Figure 5, we show the distribution on ResGCN-28. It turns out COLPER is similarly effective across samples but the perturbation distance is much smaller comparing to PointNet++, ranging from 3.5 to 6.5 (PointNet++ has the range of 11 to 25). The root cause might be that ResGCN-28 is more sensitive to color or ResGCN-28 performs better than PointNet++ (hence more vulnerable under adversarial examples). The result shows COLPER is universally effective across scenes.

Targeted Attack. Area 5 of S3IDS contains 13 classes, and we perturb the points from 6 classes, including window (label=5), door (label=6), table (label=7), chair (label=8), bookcase (label=10), and board (label=11), because the quantity of points of each class is not too small. We set the target class as wall (label=2). In the supplemental material, we provide the visual examples and all the targeted at-

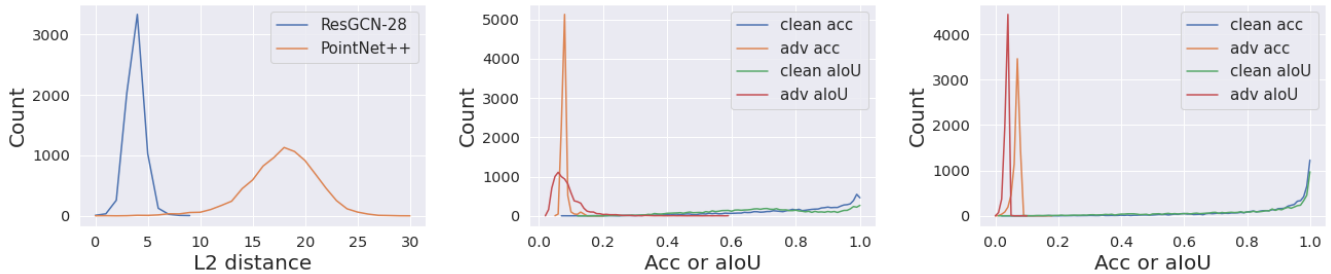


Figure 3: The L_2 distance distribution on Figure 4: The accuracy and aIoU distribution on PointNet++. Figure 5: The accuracy and aIoU distribution on ResGCN-28.

Setting	L_2	Points	SR	OOB Acc/Acc	OOB aIoU/aIoU
PointNet++(board)	5.28	49,866	93.16%	80.47%/93.97%	60.99%/74.27%
PointNet++(table)	10.55	165,155	37.70%	79.48%/86.26%	56.04%/69.09%
ResGCN-28(board)	9.69	39,552	96.08%	78.37%/88.85%	56.58%/66.43%
ResGCN-28(table)	9.29	20,136	66.43%	81.81%/91.66%	49.08%/84.80%
RandLA-Net(board)	2.37	49,806	94.29%	84.80%/85.57%	52.22%/54.06%
RandLA-Net(table)	11.82	218,496	83.10%	83.11%/83.98%	45.01%/50.58%

Table 2: The results of the targeted attack on table (label=7) and board (label=11). The results of window (label=5), door (label=6), chair (label=8), bookcase (label=10) are available in the supplementary materials. “Points” are for each class. “SR” is success rate. “OOB” is out-of-band.

tack results. Table 2 shows the segmentation results against table (label=7) and board (label=11) and the results of other labels are shown in the supplementary materials. It turns out **SR can be over 90%** for the board, when the whole three segmentation models are attacked. However, SR is much lower for other classes like the table. We speculate the reason is that the table has more complex shapes and the similarity of the object shape between the table and the wall is huge. Hence, changing these objects is deemed more difficult. In the meantime, the drop of the segmentation accuracy of the out-of-band points is moderate, mostly within 10%, which suggests COLPER is able to confine the impact to the selected source classes.

Evaluation Results on Semantic3D

Since the outdoor scenes have different properties (e.g., different object classes and larger) from the indoor scenes, we also evaluate COLPER against Semantic3D and RandLA-Net is tested.

Table 3 shows the results of the non-targeted attack. Similar as the attack against S3IDS, COLPER greatly decreases the accuracy and aIoU comparing to the baseline with the same L_2 distance: the average accuracy and aIoU drop from 70.12% and 44.8% to 11.50% and 5.77% under COLPER, while 57.09% and 27.02% for baseline. We also observe that the result on RandLA-Net has bigger variance by samples: e.g., the accuracy can drop to 0% for the best case, and 90.82% for the worst case.

As to the targeted attack, we manipulate the source points labeled as car (label=8) and try to mislead the model to predict them as man-made terrain (label=1), natural terrain

(label=2), high vegetation (label=3) and low vegetation (label=4). From Table 4, SR is near 95% when vegetation is the target class. Though outdoor scene is expected to be more complex, our result shows targeted attack is still effective. The visual example is available in the supplementary material.

Comparison to Coordinate-based Perturbation

Prior adversarial attacks against 3D point cloud all perturbed the coordinates, as described in Section. COLPER perturbs color instead. To compare them, we design a coordinate-based perturbation method for semantic segmentation, and the pseudo-code and details are shown in the supplemental material. We use PointNet++ and ResGCN-28 because RandLA-Net processes the point position features which makes the comparison not fair. Noticeably L_0 distance instead of L_2 distance for fair comparison. The coordinate-based perturbation is evaluated on ResGCN-28. We set $a = -1$ and $b = 1$ of Equation 5 to adjust the perturbation range to $[-1, 1]$.

We randomly select 200 point clouds whose segmentation accuracy is over 50% from different scenes such as office, lobby or hallway. We define another metric, *sample success rate (SSR)*, to measure the ratio of the adversarial samples that meet the L_0 criteria (i.e., less than 10% points perturbed). Our result from the supplementary materials shows color-based perturbation outperforms coordinate-based perturbation in the degradation of segmentation accuracy and aIoU (they are only counted on the successful samples). Moreover, SSR is significantly higher (81.17% versus 11.11% for ResGCN-28). In other words, **the color features**

Case	Baseline			COLPER		
	L_2	Accuracy	aIoU	L_2	Accuracy	aIoU
Best	19.31	0.00%	0.00%	19.31	0.00%	0.00%
Average	25.84	79.30%(18.95%↓)	37.22%(26.04%↓)	25.84	16.00% (82.25%↓)	7.70% (55.56%↓)
Worst	280.79	100.0%	100.0%	280.79	90.82%	25.42%

Table 3: The results of the non-targeted attack from RandLA-Net on Semantic3D.

Setting	L_2	Points	SR	OOB Acc/Acc	OOB aIoU/aIoU
RandLA-Net(man-made terrain)	10.41	31,492	85.30%	73.03%/73.64%	30.74%/33.56%
RandLA-Net(natural terrain)	5.61	11057	73.96%	84.76%/84.89%	46.63%/48.19%
RandLA-Net(high vegetation)	3.61	12,613	94.26%	97.95%/97.99%	58.86%/61.51%
RandLA-Net(low vegetation)	3.60	7,983	94.86%	74.18%/74.70%	39.57%/42.52%

Table 4: The results of the targeted attack from car (label=8) to man-made terrain (label=1), natural terrain (label=2), high vegetation (label=3), low vegetation (label=4). “Points” are for each class. “SR” is success rate. “OOB” is out-of-band.

are more vulnerable.

Attack Transferability

Existing research has shown an adversarial sample targeting image classification has transferability (Papernot, McDaniel, and Goodfellow 2016), *i.e.*, that a sample generated against one model is also effective against another model. We are interested in whether our adversarial samples have the same property. To this end, we first evaluate the attack transferability on models with different parameters. We select 400 non-targeted adversarial samples generated by COLPER on the pre-trained PointNet++, and feed them into another PointNet++ trained by ourselves (the weights and bias are different). The results shows the accuracy and aIoU on the 400 samples, suggesting our attack is transferable under different model parameters.

Then we test transferability across model families: we generate adversarial examples for ResGCN-28 and test if they can fool PointNet++. Due to different normalization steps, the adversarial samples do not directly transfer. Hence, we transform the samples and the details are in the supplementary material. Through validation on a set of normal samples, we found this transformation does not impact the segmentation results. Similarly, we select 400 samples and the result is summarized suggesting our attack is also transferrable across model families.

Noticeably, we do not transfer the attack against RandLA-Net due to its highly different approach of pre-processing. Interestingly, Xiang et al. (Xiang, Qi, and Li 2019) showed transferrability is limited no matter if the same model with different parameters or different models are tested. Our result on semantic segmentation draws an opposite conclusion.

Defenses

To mitigate the threats from the proposed adversarial attacks, gradient obfuscation, adversarial training, and anomaly detection can be tested on point cloud semantic segmentation. These ideas have been initially examined on 2D image classification and were recently migrated to 3D point cloud object recognition. For gradient obfuscation,

DUP-Net (Zhou et al. 2019) includes a denoiser layer and upsampler network structure, and GvG-PointNet++ (Dong et al. 2020) introduces gather vectors in the points clouds. However, a recent work (Sun et al. 2020) showed they are still vulnerable, due to the inherent limitation of gradient obfuscation under the white-box adaptive attacks. For adversarial training, DeepSym (Sun et al. 2020) uses a sorting-based pooling operation to overcome the issues caused by the default symmetric function. However, the robustness comes with the cost of high training overhead. For anomaly detection, (Yang et al. 2019) measured the statistics of the perturbed outputs to detect the adversarial example. Yet, none of the prior works were tested on semantic segmentation and it is unclear if they are effective for the model architecture other than CNN, e.g., GCN. As future work, we plan to evaluate these ideas on semantic segmentation.

Conclusion

In this work, we present the first study of adversarial attacks on 3D point cloud semantic segmentation. We proposed a new attack method named COLPER that imposes the perturbation on the color feature, so the attack is easier to realize in the physical world. Our evaluation on S3IDS and Semantic3D datasets shows COLPER is effective, driving down the accuracy and aIoU by a big margin, and the result is consistent across scenes and the targeted models. For the targeted attack, we observe the prominent differences between source classes, and how to make the targeted attack effective across different classes warrant future research. In addition, our evaluation shows color-based perturbation is more effective comparing to coordinate-based perturbation, and has good attack transferability. We hope with this study, more attention can be paid to make 3D point cloud semantic segmentation more robust.

References

- Arnab, A.; Miksik, O.; and Torr, P. H. 2018. On the robustness of semantic segmentation models to adversarial attacks. In *Proceedings of the IEEE Conference on Computer Vision and Pattern Recognition*, 888–897.
- Cai, M.; Sang, N.; Wang, X.; and Zhang, J. 2020. Adversarial point cloud perturbations to attack deep object detection models. In *2020 IEEE 22nd International Conference on High Performance Computing and Communications; IEEE 18th International Conference on Smart City; IEEE 6th International Conference on Data Science and Systems (HPC-C/SmartCity/DSS)*, 1042–1049. IEEE.
- Cao, Y.; Xiao, C.; Yang, D.; Fang, J.; Yang, R.; Liu, M.; and Li, B. 2019. Adversarial objects against lidar-based autonomous driving systems. *arXiv preprint arXiv:1907.05418*.
- Carlini, N.; and Wagner, D. 2017. Towards evaluating the robustness of neural networks. In *2017 IEEE Symposium on Security and Privacy (SP)*, 39–57. IEEE.
- Dong, X.; Chen, D.; Zhou, H.; Hua, G.; Zhang, W.; and Yu, N. 2020. Self-Robust 3D Point Recognition via Gather-Vector Guidance. In *Proceedings of the IEEE/CVF Conference on Computer Vision and Pattern Recognition*, 11516–11524.
- Eykholt, K.; Evtimov, I.; Fernandes, E.; Li, B.; Rahmati, A.; Xiao, C.; Prakash, A.; Kohno, T.; and Song, D. 2018. Robust physical-world attacks on deep learning visual classification. In *Proceedings of the IEEE Conference on Computer Vision and Pattern Recognition*, 1625–1634.
- Goodfellow, I. J.; Shlens, J.; and Szegedy, C. 2014. Explaining and harnessing adversarial examples. *arXiv preprint arXiv:1412.6572*.
- Hackel, T.; Savinov, N.; Ladicky, L.; Wegner, J. D.; Schindler, K.; and Pollefeys, M. 2017. Semantic3d. net: A new large-scale point cloud classification benchmark. *arXiv preprint arXiv:1704.03847*.
- Hu, Q.; Yang, B.; Xie, L.; Rosa, S.; Guo, Y.; Wang, Z.; Trigoni, N.; and Markham, A. 2020. Randla-net: Efficient semantic segmentation of large-scale point clouds. In *Proceedings of the IEEE/CVF Conference on Computer Vision and Pattern Recognition*, 11108–11117.
- Kim, J.; Hua, B.-S.; Nguyen, D. T.; and Yeung, S.-K. 2020. Minimal adversarial examples for deep learning on 3d point clouds. *arXiv preprint arXiv:2008.12066*.
- Kurakin, A.; Goodfellow, I.; and Bengio, S. 2016. Adversarial machine learning at scale. *arXiv preprint arXiv:1611.01236*.
- Landrieu, L.; and Martin, S. 2018. Large-scale Point Cloud Semantic Segmentation with Superpoint Graphs. In *2018 IEEE Conference on Computer Vision and Pattern Recognition (CVPR 2018)*. Salt Lake City, United States.
- Li, G.; Muller, M.; Thabet, A.; and Ghanem, B. 2019a. Deepgcns: Can gcns go as deep as cnns? In *Proceedings of the IEEE International Conference on Computer Vision*, 9267–9276.
- Li, J.; Chen, B. M.; and Hee Lee, G. 2018. So-net: Self-organizing network for point cloud analysis. In *Proceedings of the IEEE conference on computer vision and pattern recognition*, 9397–9406.
- Li, R.; Li, X.; Fu, C.-W.; Cohen-Or, D.; and Heng, P.-A. 2019b. Pu-gan: a point cloud upsampling adversarial network. In *Proceedings of the IEEE/CVF International Conference on Computer Vision*, 7203–7212.
- Li, Y.; Bu, R.; Sun, M.; Wu, W.; Di, X.; and Chen, B. 2018. PointCNN: Convolution on χ -transformed points. In *Proceedings of the 32nd International Conference on Neural Information Processing Systems*, 828–838.
- Liu, D.; Yu, R.; and Su, H. 2019. Extending adversarial attacks and defenses to deep 3d point cloud classifiers. In *2019 IEEE International Conference on Image Processing (ICIP)*, 2279–2283. IEEE.
- Madry, A.; Makelov, A.; Schmidt, L.; Tsipras, D.; and Vladu, A. 2017. Towards deep learning models resistant to adversarial attacks. *arXiv preprint arXiv:1706.06083*.
- Mazur, K.; and Lempitsky, V. 2020. Cloud transformers. *arXiv preprint arXiv:2007.11679*.
- Papernot, N.; McDaniel, P.; and Goodfellow, I. 2016. Transferability in machine learning: from phenomena to black-box attacks using adversarial samples. *arXiv preprint arXiv:1605.07277*.
- Qi, C. R.; Su, H.; Mo, K.; and Guibas, L. J. 2017a. Pointnet: Deep learning on point sets for 3d classification and segmentation. In *Proceedings of the IEEE conference on computer vision and pattern recognition*, 652–660.
- Qi, C. R.; Yi, L.; Su, H.; and Guibas, L. J. 2017b. Pointnet++: Deep hierarchical feature learning on point sets in a metric space. In *Advances in neural information processing systems*, 5099–5108.
- Shu, D. W.; Park, S. W.; and Kwon, J. 2019. 3d point cloud generative adversarial network based on tree structured graph convolutions. In *Proceedings of the IEEE/CVF International Conference on Computer Vision*, 3859–3868.
- Sun, J.; Koenig, K.; Cao, Y.; Chen, Q. A.; and Mao, Z. M. 2020. On the Adversarial Robustness of 3D Point Cloud Classification. *arXiv preprint arXiv:2011.11922*.
- Thomas, H.; Qi, C. R.; Deschaud, J.-E.; Marcotegui, B.; Goulette, F.; and Guibas, L. J. 2019. Kpconv: Flexible and deformable convolution for point clouds. In *Proceedings of the IEEE/CVF International Conference on Computer Vision*, 6411–6420.
- Tu, J.; Ren, M.; Manivasagam, S.; Liang, M.; Yang, B.; Du, R.; Cheng, F.; and Urtasun, R. 2020. Physically Realizable Adversarial Examples for LiDAR Object Detection. In *Proceedings of the IEEE/CVF Conference on Computer Vision and Pattern Recognition*, 13716–13725.
- Wei, J.; Lin, G.; Yap, K.-H.; Hung, T.-Y.; and Xie, L. 2020. Multi-Path Region Mining for Weakly Supervised 3D Semantic Segmentation on Point Clouds. In *Proceedings of the IEEE/CVF Conference on Computer Vision and Pattern Recognition (CVPR)*.

Wicker, M.; and Kwiatkowska, M. 2019. Robustness of 3D Deep Learning in an Adversarial Setting. *CoRR*, abs/1904.00923.

Xiang, C.; Qi, C. R.; and Li, B. 2019. Generating 3D Adversarial Point Clouds. *Proc. Computer Vision and Pattern Recognition (CVPR), IEEE*.

Xie, C.; Wang, J.; Zhang, Z.; Zhou, Y.; Xie, L.; and Yuille, A. 2017. Adversarial examples for semantic segmentation and object detection. In *Proceedings of the IEEE International Conference on Computer Vision*, 1369–1378.

Xu, Q.; Sun, X.; Wu, C.-Y.; Wang, P.; and Neumann, U. 2020. Grid-gcn for fast and scalable point cloud learning. In *Proceedings of the IEEE/CVF Conference on Computer Vision and Pattern Recognition*, 5661–5670.

Yang, J.; Zhang, Q.; Fang, R.; Ni, B.; Liu, J.; and Tian, Q. 2019. Adversarial attack and defense on point sets. *arXiv preprint arXiv:1902.10899*.

Zhao, H.; Jiang, L.; Jia, J.; Torr, P.; and Koltun, V. 2020. Point transformer. *arXiv preprint arXiv:2012.09164*.

Zhao, Y.; Zhu, H.; Liang, R.; Shen, Q.; Zhang, S.; and Chen, K. 2019. Seeing isn't believing: Towards more robust adversarial attack against real world object detectors. In *Proceedings of the 2019 ACM SIGSAC Conference on Computer and Communications Security*, 1989–2004.

Zheng, T.; Chen, C.; Yuan, J.; Li, B.; and Ren, K. 2019. Pointcloud saliency maps. In *Proceedings of the IEEE International Conference on Computer Vision*, 1598–1606.

Zhou, H.; Chen, D.; Liao, J.; Chen, K.; Dong, X.; Liu, K.; Zhang, W.; Hua, G.; and Yu, N. 2020a. LG-GAN: Label Guided Adversarial Network for Flexible Targeted Attack of Point Cloud Based Deep Networks. In *Proceedings of the IEEE/CVF Conference on Computer Vision and Pattern Recognition (CVPR)*.

Zhou, H.; Chen, D.; Liao, J.; Chen, K.; Dong, X.; Liu, K.; Zhang, W.; Hua, G.; and Yu, N. 2020b. LG-GAN: Label Guided Adversarial Network for Flexible Targeted Attack of Point Cloud Based Deep Networks. In *Proceedings of the IEEE/CVF Conference on Computer Vision and Pattern Recognition*, 10356–10365.

Zhou, H.; Chen, K.; Zhang, W.; Fang, H.; Zhou, W.; and Yu, N. 2019. DUP-Net: Denoiser and upsampler network for 3D adversarial point clouds defense. In *Proceedings of the IEEE International Conference on Computer Vision*, 1961–1970.

Supplementary Material

Symbols and Code

Symbol. Table 5 lists the symbols used in Section and their description.

Symbol	Description
x_i	a point
y_i	a class label on a point
p_i	the coordinates of x_i
c_i	the color feature of x_i
X	a point cloud
Y	the label of each point in the point cloud
\mathcal{X}	the universe of point clouds
\mathcal{Y}	the universe of class labels
F_θ	the model for segmentation
r^{color}	the perturbation values on color
$Z(\cdot)_i$	the logits of the model’s prediction
W_i	variable mapping from the feature data
T	the set of point indices
$\mathcal{D}(\cdot)$	the distance function
$S(\cdot)$	the smoothness penalty
$\mathcal{L}(\cdot)$	the loss function

Table 5: Symbols used in the paper.

Code. As the Section describes, we use the pre-trained PointNet++ (Qi et al. 2017b), ResGCN-28 under the DeepGCN family (Li et al. 2019a), and RandLA-Net (Hu et al. 2020) as the target models to evaluate COLPER, mainly because their codes and pre-trained models are publicly available¹²³. Our attack code has also been submitted, under the folder named “code”.

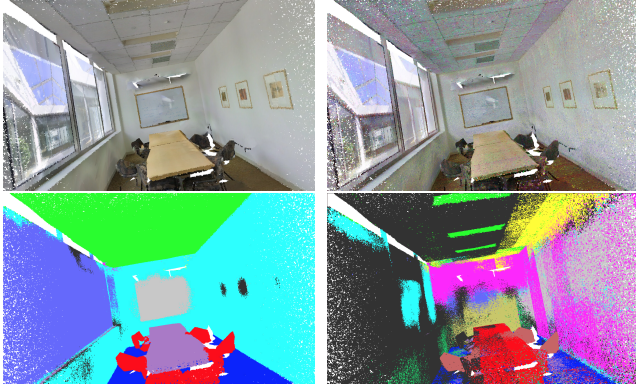


Figure 6: The non-targeted attack with Conference room 1 of Area 5 in S3DIS. The upper left, upper right, lower left, and lower right show the original scene, the perturbed scene, and the segmentation results of the original and perturbed scene.

¹PointNet++: https://github.com/yanx27/Pointnet_Pointnet2_pytorch

²ResGCN-28: https://github.com/lightaime/deep_gcns_torch

³RandLA-Net: <https://github.com/QingyongHu/RandLA-Net>

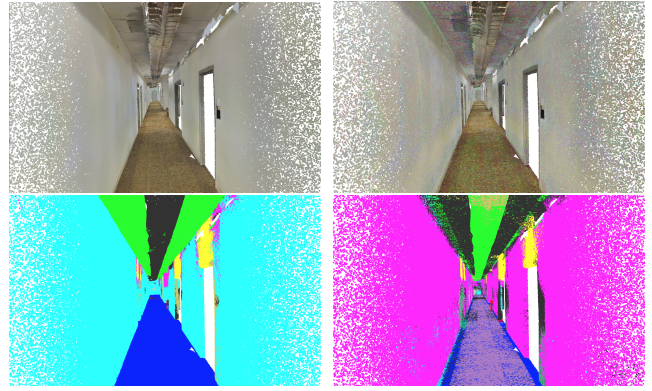


Figure 7: The non-targeted attack with Hallway 2 of Area 5 in S3DIS.

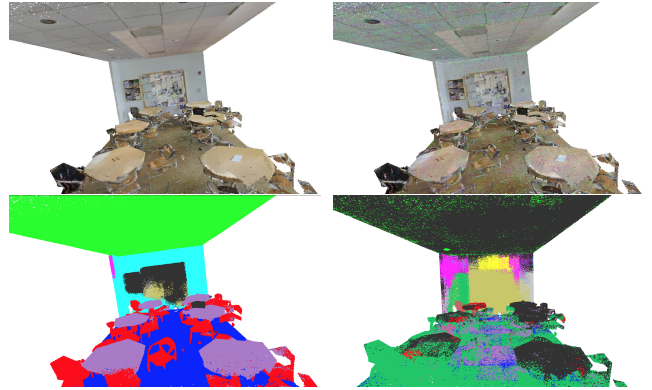


Figure 8: The non-targeted attack with Lobby 1 of Area 5 in S3DIS.

More Visualization Examples of Non-targeted Attack on S3DIS

In Section (“Non-targeted Attack”), we show a visual example to illustrate the effect of COLPER. In this section, we show more examples on different scenes like conference room, hallway and lobby. From Figure 6, Figure 7, and Figure 8, we can see the small perturbation generated by COLPER leads to prominent changes in the segmentation results.

More Results of Targeted Attack

In Section (“Targeted Attack”), we perturb the points from 6 classes, including window (label=5), door (label=6), table (label=7), chair (label=8), bookcase (label=10), and board (label=11), because the quantity of points of each class is not too small. We set the target class as wall (label=2). Due to the space limit, we only show the result about board and table in Table 2. Here we show the results of all classes in Table 6. It turns out **SR can be over 90% for window, door, bookcase, and board**, when the three segmentation models are attacked. However, SR is much lower for other classes like table and chair. We speculate the reason is that chair and table have more complex shapes. Hence, changing these ob-

Setting	L_2	Points	SR	OOB Acc/Acc	OOB aIoU/aIoU
PointNet++(window)	7.67	141,900	93.92%	53.76%/77.67%	46.59%/60.77%
PointNet++(door)	5.39	98,492	93.11%	58.54%/62.00%	45.37%/49.24%
PointNet++(table)	10.55	165,155	37.70%	79.48%/86.26%	56.04%/69.09%
PointNet++(chair)	6.69	78,866	17.63%	86.09%/90.65%	62.91%/73.19%
PointNet++(bookcase)	15.26	400,052	93.25%	52.73%/68.43%	49.63%/57.88%
PointNet++(board)	5.28	49,866	93.16%	80.47%/93.97%	60.99%/74.27%
ResGCN-28(window)	14.57	108,105	95.44%	70.88%/71.21%	39.57%/58.67%
ResGCN-28(door)	12.17	83,752	94.71%	77.96%/84.62%	65.11%/76.75%
ResGCN-28(table)	9.29	20,136	66.43%	81.81%/91.66%	49.08%/84.80%
ResGCN-28(chair)	12.62	17,213	51.63%	82.22%/83.84%	63.39%/75.59%
ResGCN-28(bookcase)	16.01	45,447	90.48%	65.10%/68.43%	55.56%/56.52%
ResGCN-28(board)	9.69	39,552	96.08%	78.37%/88.85%	56.58%/66.43%
RandLA-Net(window)	3.76	103,660	95.13%	83.98%/84.41%	50.39%/51.03%
RandLA-Net(door)	2.79	108,012	95.23%	88.42%/88.78%	49.52%/51.12%
RandLA-Net(table)	11.82	218,496	83.10%	83.11%/83.98%	45.01%/50.58%
RandLA-Net(chair)	9.06	115,997	85.98%	82.78%/82.94%	47.50%/47.94%
RandLA-Net(bookcase)	8.55	530,901	95.05%	84.02%/84.71%	50.07%/51.27%
RandLA-Net(board)	2.37	49,806	94.29%	84.80%/85.57%	52.22%/54.06%

Table 6: The results of the targeted attack on window (label=5), door (label=6), table (label=7), chair (label=8), bookcase (label=10), board (label=11). ‘‘Points’’ are for each class. ‘‘SR’’ is success rate. ‘‘OOB’’ is out-of-band.

jects is deemed more difficult. In the meantime, the drop of the segmentation accuracy of the out-of-band (OOB) points is moderate, mostly within 10%, which suggests COLPER is able to confine the impact to the selected source classes.

Here we also visualize another example about the targeted attack in Figure 9. We set PointNet++ as the target model, and the board as the source class. Since most of its points are classified as wall after the attack, COLPER could make the board ‘‘disappear’’ in the view of the segmentation model.



Figure 9: The targeted attack with Office 33 of Area 5 in S3DIS.

Targeted Attack against Multiple Classes. In Section ‘‘Targeted Attack’’, we reported the result of targeted attack against a single class. Here we evaluate whether COLPER is effective when multiple source classes are perturbed. One example is visualized in Figure 10. We consider table (label=7), chair (label=8), bookcase (label=10) as the source classes to be changed, and PointNet++ as

the segmentation model. The result shows they are all misclassified as wall by the segmentation model.

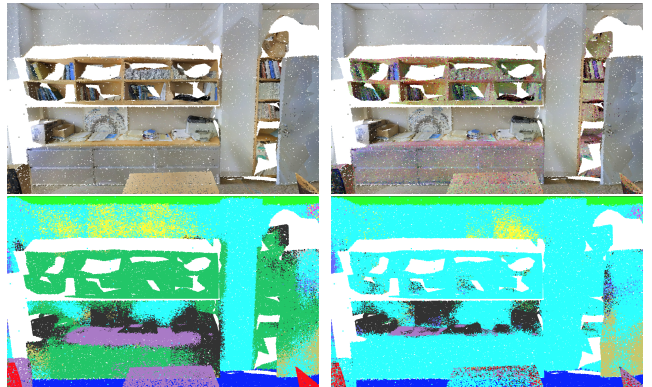


Figure 10: The targeted attack against multiple source classes in Office 33 of Area 5 in S3DIS. Table, chair and bookcase are all mis-classified as wall after the attack.

Comparison to Coordinate-based Perturbation

In Section , we briefly describe how we compare color-based and coordinate-based perturbation. Here we describe more details. We adjusted the pseudo-code of COLPER to ensure the fair comparison, shown in Algorithm 2, Essentially, we use L_0 distance, *i.e.*, how many points are changed, for $\mathcal{D}(r_{color})$. We set of a maximum threshold of L_0 distance to 10% of the whole points. Using L_0 ensures fair comparison, since other distance metrics like L_2 and L_∞ yield different values ranges for color and coordinate.

Another change over Algorithm 1 is to select a set of most impactful points and only perturb them, such that the L_0 cri-

teria can be met. Specially, in each iteration i , we assume the points allowed to be perturbed is X_i (e.g., 4,096 points for S3IDS dataset). After perturbation, the N least impactful points X_N are selected, and the point cloud is restored. The next iteration $i + 1$, the perturbation will be only executed on a subset of X_i , or $X_{i+1} = X_i \setminus X_N$. When the remaining points that can be perturbed are less than 10% after a number of iterations, the point cloud will be perturbed without restoration. The equation below shows how the N points are selected.

$$N = \arg \min_N g_N \cdot r_N \quad (9)$$

where g_N is the gradient and r_N means the perturbation value. We set N to 100 during experiment. Below we show the adjusted version.

Our result in Table 7 shows color-based perturbation outperforms coordinate-based perturbation in the degradation of segmentation accuracy and aIoU (they are only counted on the successful samples). Moreover, sample success rate (SSR) is significantly higher (81.17% versus 11.11% for ResGCN-28). In other words, **the color features are more vulnerable**.

Setting	Accuracy	aIoU	SSR
ResGCN-28 (Color)	6.84%	3.55%	81.17%
ResGCN-28 (Coordinate)	18.11%	9.96%	11.11%
PointNet++ (Color)	12.20%	12.05%	85.77%
PointNet++ (Coordinate)	N/A	N/A	N/A

Table 7: The results of the L_0 non-targeted attack on ResGCN-28 and PointNet++.

Setting		Accuracy	aIoU
PointNet++	Pre-trained	7.24%	9.44%
	Self-trained	34.35%	31.39%
ResGCN-28		7.11%	3.68%
PointNet++		39.01%	25.30%

Table 8: The upper row shows the results of attack transferability on PointNet++. The lower row displays the results from ResGCN-28 to PointNet++.

More Details of Attack Transferability

Here we extend our method description and evaluation result of Section . We tested the attack transferability on different model parameters and model families. For the latter case, we use the adversarial example generated against ResGCN-28 to attack PointNet++. But due to different normalization steps (i.e., the coordinate ranges in $[-1, 1]$ for ResGCN-28 while $[0, 3]$ for PointNet++), the adversarial samples do not directly transfer. Hence, we transform the samples with Equation 10 before they are fed into PointNet++.

$$X = \left\{ pos_x = 2 * pos_x, pos_y = 2 * pos_y, pos_z = \frac{3}{2} * pos_z + \frac{3}{2} \right\} \quad (10)$$

We compute the accuracy and aIoU in the two settings, and the results suggest our attack is transferable when the model parameters differ and model families differ (Table 8).

Visualization Examples of Non-targeted Attack on Semantic3D

As the Section described, COLPER greatly decreases the accuracy and aIoU comparing to the baseline with the same L_2 distance: the average accuracy and aIoU drop from 70.12% and 44.8% to 11.50% and 5.77% under COLPER, while 57.09% and 27.02% for baseline. Figure 11 shows a visual example of a scene in the Semantic3D.

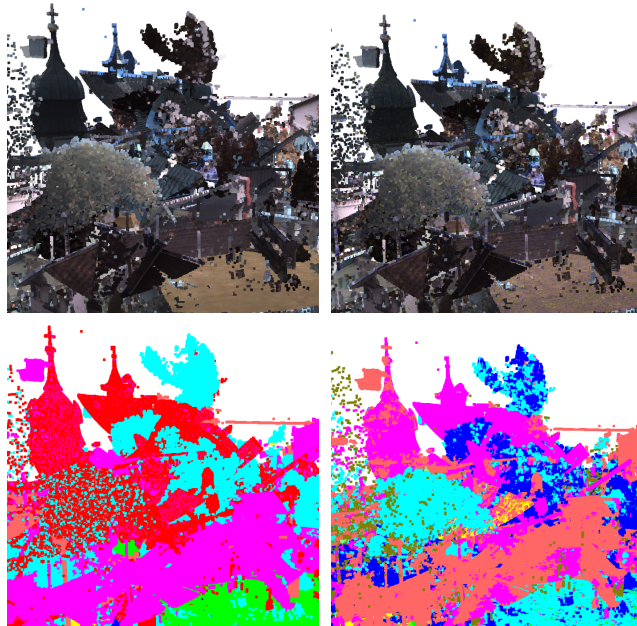


Figure 11: The non-targeted attack in Semantic3D. The upper left, upper right, lower left, and lower right show the original scene, the perturbed scene, and the segmentation results of the original and perturbed scene.

Algorithm 2: The pseudo-code of coordinate-based attack.

Input: The type of perturbation

$tar = \{s | s \in \{color, coordinate\}\}$, the original point cloud X , the ground-truth labels Y_{gt} , the maximal number of iterations $Steps$, the target labels Y_t , the top α nearest neighbors, the learning rate lr , the fixed-point mask with the same shape of the point cloud $M = \{m_i \in \{True, False\}\}$, the identity matrix \mathbb{I}

Output: the adversarial perturbation r

$X_0 \leftarrow X, r \leftarrow X^{tar}, i \leftarrow 1, M \leftarrow \mathbb{I};$

if $tar == color$ **then**

$w = \tanh^{-1}(2 \cdot r - 1);$

else if $tar == coordniate$ **then**

$w = \tanh^{-1}(r);$

while $M.sum > X.point_{num} \cdot 1\%$ **do**

while $i \leq Steps$ **do**

if $tar == color$ **then**

$X_i^{pertub} = \frac{1}{2} \tanh(w) + 1;$

else if $tar == coordniate$ **then**

$w = \tanh^{-1}(pertub);$

$r = X_i^{pretub} - X_{i-1}^{pertub};$

$X_i = X_{i-1} + r;$

if targeted attack **then**

$loss = \mathcal{L}_t(X_i, Y_t);$

else if non-targeted attack **then**

$loss = \mathcal{L}_{nt}(X_i, Y_{gt});$

$gain_i = loss;$

$r, g = Update(gain_i, lr);$

if $Converge(gain_i)$ **then**

return ;

else if $(i \% (int(Steps * 0.01)) == 0) \&$

$(gain_i \geq gain_{i-1})$ **then**

$r_{pertub} = r_{pertub} + \text{uniform noise};$

$i \leftarrow i + 1;$

end

$N = \arg \min_{100} g \cdot r;$

$M = Fix(M, N);$

end

return $M, r_{color};$
